

## Annealing of electron-induced defects in *n*-type germanium

P. M. Mooney,\* F. Poulin, and J. C. Bourgoin

*Groupe de Physique des Solides de l'École Normale Supérieure,  
Université de Paris VII, tour 23, 2 place Jussieu,  
F-75251 Paris Cedex 05, France*

(Received 14 June 1982; revised manuscript received 26 January 1983)

*n*-type,  $10^{13}$  and  $2 \times 10^{15}$   $\text{cm}^{-3}$  doped germanium has been irradiated with  $\sim 1$ -MeV electrons at liquid-helium and room temperatures. With the use of transient-capacitance spectroscopy, six electron traps and one hole trap were observed following irradiation at 4 K. Their energy levels have been determined to be at  $E_c - 40, 120, 120, 260, 390,$  and  $530$  meV, and at  $E_v + 250$  meV. The isochronal annealing behavior of these traps, in addition to that of the four electron traps and of the four hole traps produced by room-temperature irradiation, has been studied in detail. Comparison of our results with previously published ones indicates that (i) the divacancy anneals around  $150^\circ\text{C}$  and the *E* center around  $100^\circ\text{C}$ , (ii) the two levels at  $E_c - 120$  meV are associated with the germanium interstitial or complexes involving a germanium interstitial, and (iii) there appears to be a vacancy level in the range  $100$ – $200$  meV from the conduction band, which anneals at  $\sim 100$  K.

### I. INTRODUCTION

Because it has not yet been possible to identify defects in germanium using electron paramagnetic resonance, attempts to identify defects in this material have involved indirect methods. In the case of irradiation-induced defects, one approach has been to correlate the defect introduction and annealing rates with the nature and concentration of the impurities present in the material. For instance, a defect which anneals around  $100^\circ\text{C}$  has been tentatively identified as the *E* center (vacancy-doping impurity complex) because its introduction rate increases with the concentration of the dopant impurity<sup>1</sup> and because its precise annealing temperature varies slightly with the nature of this impurity.<sup>2</sup> Previously, these rates could only be obtained from conductivity measurements, the concentration of a defect being monitored by the free-carrier recovery in the various annealing stages. Unfortunately, the results of such annealing studies are often unclear or confusing when several defects anneal in the same temperature range. As it will be shown in this paper, this is the case for four electron traps and four hole traps which anneal in the temperature range  $100$ – $200^\circ\text{C}$ . It is thus necessary to use a more precise spectroscopic technique, i.e., one based on the analysis of a capacitance transient, which allows a direct measurement of the introduction and annealing rates of each defect separately.

In this paper, we describe the annealing behavior

of the traps which were observed following electron irradiation at liquid-helium and room temperatures using deep-level transient spectroscopy (DLTS). The characteristics of five majority carrier traps (labeled  $E_1$  to  $E_5$ ) and four minority carrier traps (labeled  $H_1$  to  $H_4$ ) produced by room-temperature irradiation have already been described.<sup>3–5</sup> Their introduction rates as a function of the energy of irradiation have been determined previously.<sup>4,6</sup> This paper is thus restricted to the description of their annealing behavior. We also describe the annealing behavior of the traps which are observed following irradiation at 4.2 K. The energy levels of most of these traps, which we label  $M_1$ – $M_7$  are also given here.

The results presented here confirm that the defects which are stable at room temperature are not primary defects but complexes resulting from the association of primary defects with themselves (divacancy) and of impurities with primary defects (vacancies and interstitials) which are unstable in the range  $60$ – $200$  K.<sup>7</sup>

### II. EXPERIMENTAL DETAILS

Two kinds of *n*-type material were used in this study. Commercial  $p^+n$  diodes of material *A*,  $10^{13}$   $\text{cm}^{-3}$  doped, were used for annealing studies following room-temperature irradiation. This same material and material *B* with higher dopant concentration ( $2 \times 10^{15}$   $\text{cm}^{-3}$ , Sb doped) were used for an-

nealing studies following irradiation at 4 K. Diodes made from material *B* were fabricated by Ga diffusion (16 h at 830°C). The electrical contacts were made by Ni evaporation, followed by electrolytic deposition of gold and a 300°C heat treatment. Apparently, such treatment does not induce defects which are observable with the DLTS technique.

The samples were irradiated with 0.5-, 1-, 1.5-, and 2-MeV electrons at fluences ranging from  $10^{13}$  to  $10^{15}$  cm $^{-2}$ . The electron beam was scanned on a surface larger than the area of the sample in order to insure the uniformity of the dose. Irradiations at liquid-helium temperature were done as described in Ref. 8. Annealing in the range 4–300 K was performed *in situ* while annealing above room temperature was done in a furnace at  $10^{-6}$  Torr pressure. The capacitance transients were measured using either a double boxcar<sup>9</sup> or a two-phase lock-in detector.<sup>10</sup>

### III. IRRADIATION AT LIQUID-HELIUM TEMPERATURE

The DLTS spectrum of material *A* irradiated with 1-MeV electrons at 4.2 K shows five electron traps which we labeled  $M_2$ ,  $M_3$ ,  $M_4$ , and  $E_2$  and one hole trap  $H_2$  (see Fig. 1). The peak labeled  $M_1$  in Fig. 1 was present before irradiation and its concentration is not modified by the irradiation. The hole trap  $H_2$  often masks the electron trap  $M_4$  when the dose of irradiation is too small, i.e., when the  $M_4$  concentration is low. The concentrations of the electron traps following two irradiations with  $4 \times 10^{14}$  and  $7.2 \times 10^{14}$  cm $^{-2}$  are given in Table I.

Similar spectra are obtained in material *B*. In this case, 1.5-MeV electrons were used with fluences ranging from  $4 \times 10^{15}$  to  $6 \times 10^{15}$  cm $^{-2}$ . The only difference between the spectra of the two materials is the existence of two new traps, labeled  $M_7$  (which probably masks  $M_4$ ) and  $M_6$  (see Fig. 1). Trap  $M_7$  is not seen in material *A* presumably because some

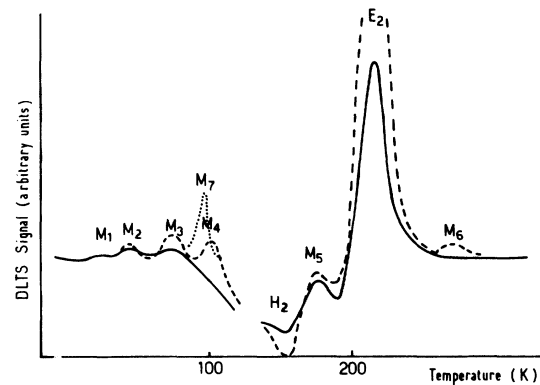


FIG. 1. DLTS spectra obtained in material *A* following irradiation at 4 K with  $4 \times 10^{14}$  (solid line) and  $7.2 \times 10^{14}$  (dashed line) 1-MeV electrons/cm $^2$ . The dotted lines indicate the additional two peaks which are observed in material *B* following  $2 \times 10^{15}$  1.5-MeV-electrons/cm $^2$  irradiation. The conditions of observation are the following: emission rate 22.2 s $^{-1}$ , reverse bias 3 V, pulse amplitude 2.8 V, and pulse width 250  $\mu$ s.

annealing had occurred at a temperature lower than the temperature at which it could be observed (owing to the chosen emission rate). The concentrations of the electron traps obtained for these irradiations are also given in Table I.

The energy levels associated with traps  $M_2$  to  $M_6$ ,  $E_2$ , and  $H_2$  have been determined by studying the variation of their emission rates with temperature. The data given in Figs. 2–4 were used to determine the energy levels. These levels are at  $E_c - 40$ , 120, 120, 260, 390, and 530 meV and  $E_v + 250$  meV for traps  $M_2$  to  $M_6$ ,  $E_2$ , and  $H_2$ , respectively. Since trap  $M_7$  anneals at nearly the same temperature at which it is observed (this may be the reason that  $M_7$  was not observed in material *A*), it was not possible to determine its energy level exactly; however, it appears to be between 100 and 200 meV below the conduction band. Table I indicates the introduction

TABLE I. Concentrations (cm $^{-3}$ ) and introduction rates  $\nu$  of the traps observed in the two materials following two doses of irradiation at 1 MeV (material *A*) and 1.5 MeV (material *B*).

Material	<i>A</i> ( $10^{13}$ cm $^{-3}$ )			<i>B</i> ( $2 \times 10^{15}$ cm $^{-3}$ ), Sb doped			
	Fluence (cm $^{-2}$ )	$4 \times 10^{14}$	$7.2 \times 10^{14}$	$4 \times 10^{15}$	$6 \times 10^{15}$	$\nu_B$ (cm $^{-1}$ )	
$M_2$		$4 \times 10^9$	$6 \times 10^9$	$9 \times 10^{-6}$	$4 \times 10^{12}$	$5 \times 10^{12}$	$1 \times 10^{-3}$
$M_3$		$6 \times 10^9$	$1.2 \times 10^{10}$	$1.6 \times 10^{-5}$	$1.3 \times 10^{13}$	$1.5 \times 10^{13}$	$3.5 \times 10^{-3}$
$M_4$			$3 \times 10^{10}$	$4.1 \times 10^{-5}$			
$M_5$		$1.8 \times 10^{10}$	$2.1 \times 10^{10}$	$4.0 \times 10^{-5}$	$6 \times 10^{12}$	$10^{13}$	$1.5 \times 10^{-3}$
$E_2$		$1.2 \times 10^{11}$	$2.3 \times 10^{11}$	$3.1 \times 10^{-4}$	$1.2 \times 10^{14}$	$1.9 \times 10^{14}$	$3 \times 10^{-2}$
$M_7$						$3 \times 10^{13}$	$5 \times 10^{-3}$
$M_6$					$3 \times 10^{12}$	$5 \times 10^{12}$	$8 \times 10^{-4}$

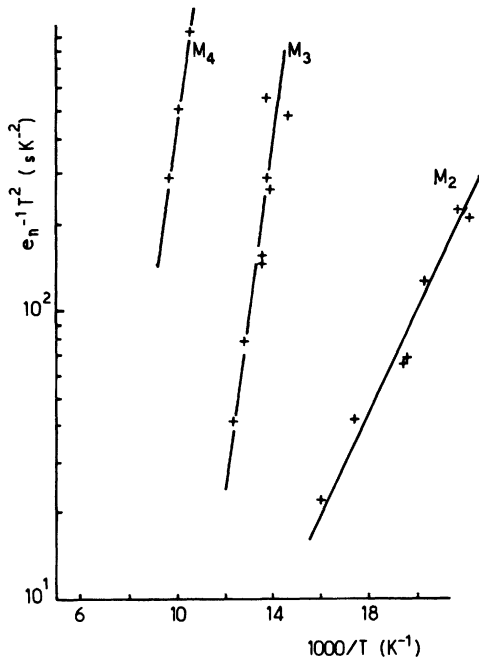


FIG. 2. Variation of the emission rate (corrected for the temperature dependence of the carrier velocity and of the density states in the band) vs temperature for the  $M_2$ ,  $M_3$ , and  $M_4$  traps.

rates  $v_A$  and  $v_B$  ( $\text{cm}^{-1}$ ), for materials  $A$  and  $B$ , respectively, of all the observed traps and shows that  $v_B/v_A \approx 10^2$ . This result is in agreement with early conductivity measurements, which indicated that the lower the doping level the smaller the introduction rate.<sup>11,13</sup>

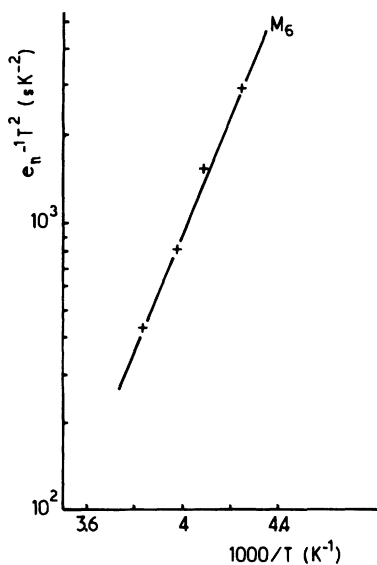


FIG. 3. Variation of the emission rate (corrected for the temperature dependence of the carrier velocity and of the density states in the band) vs temperature for the  $M_6$  trap.

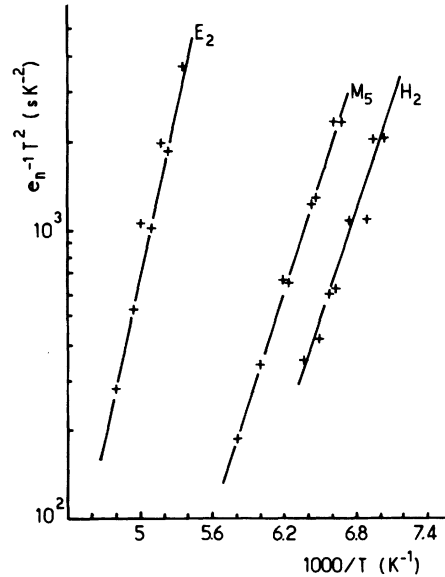


FIG. 4. Variation of the emission rate (corrected for the temperature dependence of the carrier velocity and of the density states in the band) vs temperature for the  $M_5$ ,  $E_2$ , and  $H_4$  traps.

The carrier removal at 4 K, measured from the capacitance-voltage characteristics before and after irradiation, is of the order of  $\sim 10^{12} \text{ cm}^{-1}$  in material  $A$ . For instance,  $1.8 \times 10^{-2} \text{ cm}^{-3}$  carriers disappeared following irradiation with  $4 \times 10^{14}$  electrons  $\text{cm}^{-2}$ . When compared to the sum of the introduction rates of all the traps  $\sim 10^{-3} \text{ cm}^{-1}$ , this value implies that  $\sim 90\%$  of the created defects were not observed. Part of these defects are believed to be the vacancies and interstitials which remain paired and which recombine at 65 K.<sup>11-13</sup> Indeed, we observed that 35% of the carriers were recovered after annealing at 65 K. Presumably, the measured concentration for the  $M_7$  trap, which anneals at about 100 K (the temperature at which it is observed) is not the initial concentration but the concentration after some annealing has already occurred. After further annealing, the carrier concentration recovers again:  $\sim 10\%$  after 120 K annealing and an additional  $\sim 10\%$  after annealing at 310 K. Thus, a total carrier recovery of  $\sim 55\%$  occurs upon annealing at room temperature. The detailed annealing behavior of all the traps observed is shown in Fig. 5. Materials  $A$  and  $B$  show similar behavior. Typically,  $M_7$  anneals around 100 K,  $M_2$  around 160 K, and  $M_3$  and  $M_5$  in the range of 160–220 K.

#### IV. IRRADIATION AT ROOM TEMPERATURE

Room-temperature irradiation results in the introduction of five electron traps ( $E_1-E_5$ ) and four hole

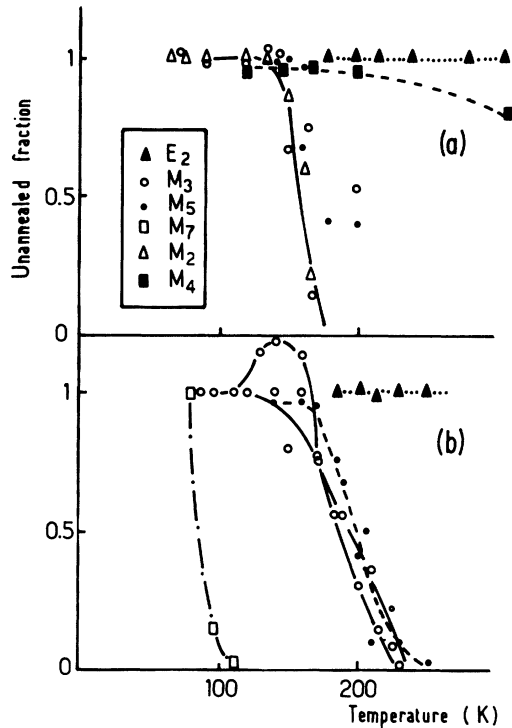


FIG. 5. Variation with isochronal annealing temperature of the concentration of the various traps observed following irradiation at 4 K: (a) in material A (1 MeV) and (b) in material B (1.5 MeV).

traps ( $H_1$ – $H_4$ ) whose relative introduction rates vary with the energy of irradiation (see Fig. 6). The electrical characteristics of these traps, as well as the

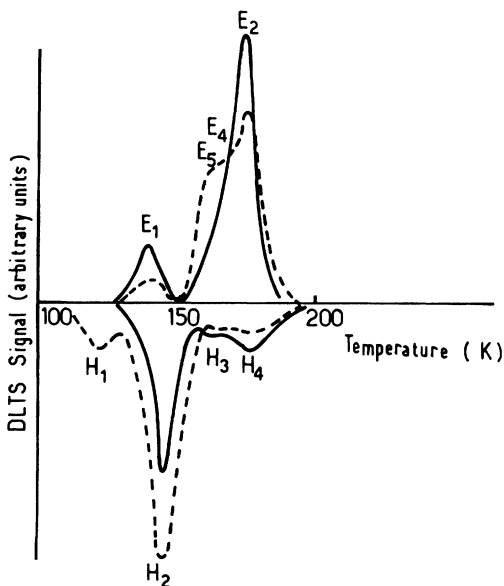


FIG. 6. DLTS spectra showing the electrons and hole traps observed following room-temperature irradiation. The solid lines correspond to irradiation with low-energy electrons (typically 0.5 MeV) and the dashed lines to irradiation with high-energy electrons (typically 2 MeV).

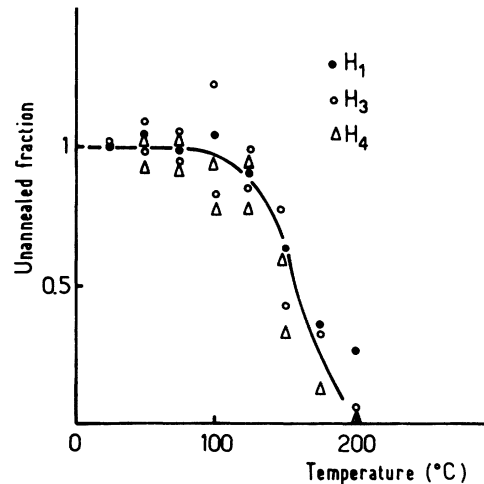


FIG. 7. Unannealed fraction of traps  $H_1$ ,  $H_3$ , and  $H_4$  vs isochronal annealing temperature for 1- or 2-MeV irradiations.

measurements of their introduction rates, have been reported elsewhere,<sup>4,6</sup> so we present only their annealing behavior here.

Trap  $E_3$ , which anneals at room temperature, i.e., just at the temperature it is created, has not yet been studied. The isochronal annealing behavior of the  $H_1, H_3, H_4$  traps, the  $H_2$  trap, the  $E_1$  and  $E_2$  traps,

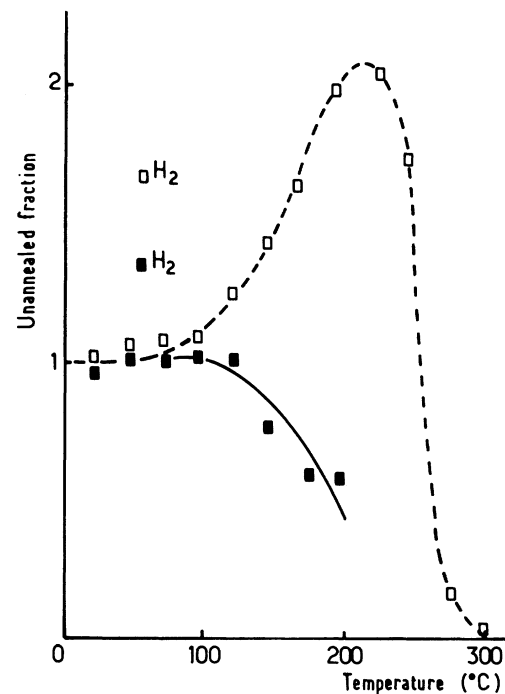


FIG. 8. Unannealed fraction of traps  $H_2$  vs isochronal annealing temperature. The solid line corresponds to irradiation with low-energy electrons (1 MeV), the dashed line to irradiation with high-energy electrons (2 MeV).

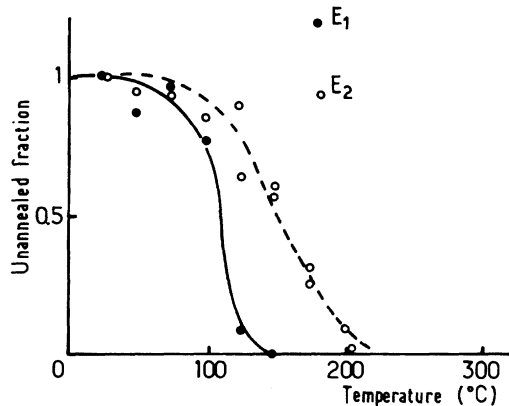


FIG. 9. Unannealed fraction of traps  $E_1$  and  $E_2$  vs isochronal annealing temperature for 1- or 2-MeV irradiations.

and the  $E_4$  and  $E_5$  traps, is shown in Figs. 7, 8, 9, and 10, respectively. Note that the annealing behavior of  $E_4$ ,  $E_5$ , and  $H_2$  (Figs. 8 and 10), which as we shall see in Sec. V are related to the divacancy, depends on the energy of irradiation, i.e., on the relative concentrations of vacancies and divacancies. The annealing behavior of the traps shown in Figs. 7 and 9 is independent of the energy of irradiation.

## V. DISCUSSION

The vacancy-interstitial pairs produced by the irradiation at 4 K are believed to be stable up to 65 K in doped  $n$ -type germanium for the following reasons: In heavily doped material the defect introduction rate is comparable to the theoretical one<sup>13</sup>

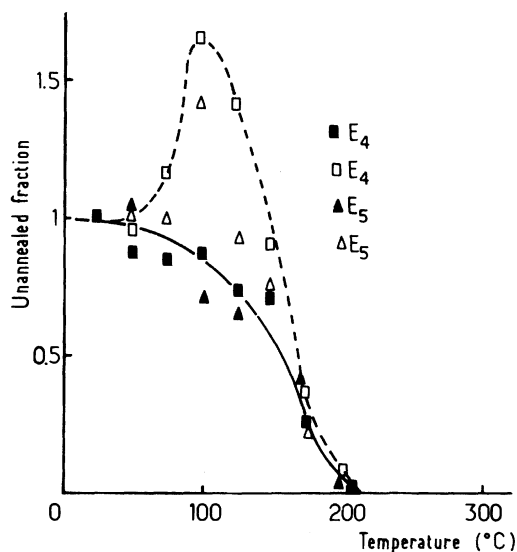


FIG. 10. Unannealed fraction of traps  $E_4$  and  $E_5$  vs isochronal annealing temperature. The solid line corresponds to a low-energy irradiation and the dashed line to a high-energy irradiation.

and nearly 100% of the defects disappear at 65 K (Ref. 11); moreover, the annealing kinetics are characteristic of pair recombination.<sup>12</sup> In lightly doped material, a decrease of the defect introduction rate is observed which can only be explained by the mobility of the interstitial introduced by the irradiation (as is true in silicon) resulting in partial recombination of the pairs.<sup>11,13</sup> As discussed in detail in Ref. 15, this behavior of the interstitial can be understood in terms of an ionization-induced mobility: Hole trapping induces the jump of the interstitial from one site to a neighboring one. Thus, the lower the  $n$ -doping concentration, the higher the interstitial mobility. From the effect of light, which shifts the 65-K annealing stage to lower temperatures,<sup>12</sup> it can be deduced that recombination of the vacancy-interstitial pairs at 65 K occurs through the interstitial mobility.

Consequently, the defects we observe just above the temperature at which pairs recombine, must be either the element of the pair which is not yet mobile, i.e., the vacancy, or complex defects resulting from the association of interstitials with impurities. When the vacancy becomes mobile, complex defects formed by the association of vacancies with themselves (divacancies) and with impurities should also be present.

The first annealing stage following vacancy-interstitial pair recombination occurs at  $\sim 100$  K. At this temperature, Whan<sup>16</sup> observed the growth of ir bands (at 736 and 819  $\text{cm}^{-1}$ ) associated with an oxygen related defect. She suggested that this defect is a vacancy-oxygen complex (the  $A$  center), with its growth being due to the vacancy mobility at this temperature. In this view, the traps we observed above 65 K cannot be attributed to vacancy-interstitial pairs. Because trap  $M_7$  anneals at practically the same temperature as the growth of the oxygen complexes occurs, it could be the vacancy. Traps  $M_2$  and  $M_3$ , which are probably associated with the same defect since they are always found in equal concentration and have identical annealing behavior are very likely to be an interstitial related defect since they are observed below 100 K. This conclusion is in agreement with another of Whan's observations<sup>16</sup>; namely that a partial recovery of the  $A$  center occurs around 200 K because it is induced by the annealing of an interstitial related defect.

As for trap  $M_5$ , its annealing behavior correlates with the annealing of the 2.4- $\mu\text{m}$  ir absorption band reported by Stein<sup>17</sup> and Morrison and Newman.<sup>18</sup> Stein suggested this band is due to the divacancy. This cannot be the case, however, because the trap  $M_5$  has a different "signature" (variation of the emission rate with temperature) than traps  $E_4$  or  $E_5$  which we have already demonstrated are associated

with the divacancy.<sup>6</sup> Traps  $E_4$ ,  $E_5$ , and  $H_1$  are believed to be associated with the divacancy for the following reason: The variations of their introduction rates (always found to be equal) induced by electron irradiation, are characteristic of a threshold energy which is approximately two times the threshold energy for atomic displacement.<sup>4,6</sup> The annealing behavior of these three traps is the same confirming that they correspond to the same defect.

The identification of  $E_1$  with the  $E$  center (vacancy-doping impurity complex) can be made on the following grounds: It has the same annealing behavior and the same energy level as a defect which has been identified as the  $E$  center (vacancy-doping impurity complex) because its introduction rate increases with the doping impurity<sup>1</sup> and its annealing behavior and energy level position vary slightly with the nature of this doping impurity.<sup>2</sup>

Finally, the  $H_2$  trap has the same annealing behavior as the 772- and 819-cm<sup>-1</sup> ir bands associated with a defect containing oxygen.<sup>16</sup> The  $H_3$ ,  $H_4$ , and  $E_2$  traps are also probably associated with a defect containing oxygen since they exhibit the same annealing behavior as the 715- and 808-cm<sup>-1</sup> absorption bands<sup>16</sup> and an EPR spectrum<sup>19</sup> associated with an oxygen complex. It is not possible to decide if the  $H_2$  and  $E_2$  traps are related to interstitial or vacancy-oxygen complexes since they are observed

only for temperatures higher than the annealing temperature of the vacancy. However, since the concentration of  $H_2$  traps seems to be increased by vacancy dissociation (in case of low-energy irradiation), this indicates that this defect contains a vacancy in addition to oxygen.

## VI. CONCLUSION

The use of a spectroscopic technique has allowed us to obtain detailed information on the annealing behavior of the numerous defects introduced by electron irradiation in *n*-type germanium. After the recombination of vacancy-interstitial pairs at about 65 K, the annealing of a trap tentatively identified as the vacancy was observed at 100 K. Another defect, observed prior to the annealing of the vacancy, is believed to be a complex which includes a germanium interstitial. The annealing of traps believed to be complexes of vacancies with oxygen and with the dopant impurity as well as the divacancy was also observed.

## ACKNOWLEDGMENTS

We wish to thank Thomson-CSF for financial support for one of us (P.M.M.) during 1979–1980 under Contract No. DRET 79.34.374. The Groupe des Solides de l'École Normale Supérieure is Laboratoire associé au Centre National de la Recherche Scientifique.

\*Permanent address: IBM Thomas J. Watson Research Center, P.O. Box 218, Yorktown Heights, N.Y. 10598.

<sup>1</sup>J. C. Pigg and J. H. Crawford, Jr., Phys. Rev. **135**, A1141 (1964).

<sup>2</sup>H. Saito, J. C. Pigg, and J. H. Crawford, Jr., Phys. Rev. **144**, 725 (1966).

<sup>3</sup>P. M. Mooney, M. Cherki, and J. C. Bourgoin, J. Phys. (Paris) Lett. **40**, L19 (1979).

<sup>4</sup>F. Poulin and J. C. Bourgoin, in *Recent Developments in Condensed Matter Physics*, edited by J. T. Devreese (Plenum, New York, 1981), Vol. 3, p. 83.

<sup>5</sup>F. Poulin and J. C. Bourgoin, Phys. Rev. B **26**, 6788 (1982).

<sup>6</sup>F. Poulin and J. C. Bourgoin, Rev. Phys. App. **15**, 15 (1980).

<sup>7</sup>For a review, see T. V. Mashovets, in *International Conference on Radiation Effects in Semiconductors, Dubrovnik, 1976*, edited by N. B. Urli and J. W. Corbett (The Institute of Physics, London, 1977), p. 30.

<sup>8</sup>J. C. Bourgoin, J. Zizine, S. Squelard, and P. Baruch, Rad. Eff. **2**, 287 (1969).

<sup>9</sup>D. V. Lang, J. Appl. Phys. **45**, 3023 (1974).

<sup>10</sup>D. Pons, P. M. Mooney, and J. C. Bourgoin, J. Appl.

Phys. **51**, 2038 (1980).

<sup>11</sup>T. A. Callcott and J. W. MacKay, Phys. Rev. **161**, 698 (1967).

<sup>12</sup>J. Zizine, in *Radiation Effects in Semiconductors*, edited by F. L. Vook (Plenum, New York, 1968), p. 188.

<sup>13</sup>J. Bourgoin and F. Mollott, Phys. Status Solidi B **43**, 343 (1971).

<sup>14</sup>J. C. Bourgoin, P. M. Mooney, and F. Poulin, in *Defects and Radiation Effects in Semiconductors, 1980*, edited by R. R. Hasiguti (The Institute of Physics, London, 1981), p. 33.

<sup>15</sup>J. C. Bourgoin and M. Lannoo, *Point Defects in Semiconductors, II—Experimental Aspects* (Springer, Berlin, 1983).

<sup>16</sup>R. E. Whan, Phys. Rev. **140**, A690 (1965).

<sup>17</sup>H. J. Stein, in *International Conference on Radiation Damage and Defects in Semiconductors, Reading, England, 1972* (The Institute of Physics, London, 1973), p. 315.

<sup>18</sup>S. R. Morrison and R. C. Newman, J. Phys. C **6**, 1981 (1973).

<sup>19</sup>J. A. Baldwin, Jr., J. Appl. Phys. **36**, 793 (1965).